Published in final edited form as:
Mol Pharm. 2011 August 1; 8(4): 1292–1302. doi:10.1021/mp2001022.

Synthesis and characterization of a BODIPY conjugate of the BCR-ABL kinase inhibitor Tasigna® (Nilotinib): Evidence for transport of Tasigna® and its fluorescent derivative by ABC drug transporters

Suneet Shukla[1], **Amanda P. Skoumbourdis**[2], **Martin J. Walsh**[2], **Anika M.S. Hartz**[3], **King Leung Fung**[1], **Chung-Pu Wu**[1], **Michael M. Gottesman**[1], **Björn Bauer**[4], **Craig J. Thomas**[2], and **Suresh V. Ambudkar**[1,*]

[1]Laboratory of Cell Biology, Center for Cancer Research, National Cancer Institute, NIH, Bethesda, MD 20892

[2]NIH Chemical Genomics Center, 9800 Medical Center Drive, Rockville, MD 20850

[3]Department of Biochemistry and Molecular Biochemistry, Medical School, University of Minnesota, Duluth, MN 55812

[4]Department of Pharmaceutical Sciences, College of Pharmacy, University of Minnesota, Duluth, MN 55812

Abstract

Tasigna® (Nilotinib) is a recently approved BCR-ABL kinase inhibitor by the Food and Drug Administration, which is indicated for the treatment of drug-resistant chronic myelogenous leukemia (CML). The efflux of tyrosine kinase inhibitors by ATP-binding cassette (ABC) drug transporters, which actively pump these drugs out of cells utilizing ATP as an energy source, has been linked to the development of drug resistance in CML patients. We report here synthesis and characterization of a fluorescent derivative of Tasigna to study its interaction with two major ABC transporters, P-glycoprotein (Pgp) and ABCG2, in *in vitro* and *ex vivo* assays. A fluorescent derivative of Tasigna, BODIPY® FL Tasigna, inhibited the BCR-ABL kinase activity in K562 cells and was also effluxed by Pgp- and ABCG2-expressing cells in both cultured cells and rat brain capillaries expressing Pgp and ABCG2. In addition, [^{3}H]-Tasigna was also found to be transported by Pgp-expressing polarized LLC-PK1 cells in a transepithelial transport assay. Consistent with these results, both Tasigna and BODIPY® FL Tasigna were less effective at inhibiting the phosphorylation of Crkl (a substrate of BCR-ABL kinase) in Pgp- and ABCG2-expressing K562 cells due to their reduced intracellular concentration. Taken together, these data provide evidence that BODIPY® FL Tasigna is transported by Pgp and ABCG2, and Tasigna is transported by Pgp. Further, we propose that BODIPY® FL Tasigna can potentially be used as a probe to study Tasigna in imaging Pgp- and/or ABCG2- expressing cancer cells and other preclinical studies.

Keywords

ABC transporter; ABCG2; BCR-ABL kinase; multidrug resistance; P-glycoprotein; Tasigna

[*]Corresponding author: Suresh V. Ambudkar, Laboratory of Cell Biology, National Cancer Institute, NIH, Bethesda, MD 20892-4256, USA; Tel: 301-402-4178; Fax: 301-435-8188; ambudkar@helix.nih.gov.

Supporting Information (SI). Synthesis and characterization of BODIPY® FL Tasigna and its intermediates. This information is available free of charge via the Internet at http://pubs.acs.org/.

Introduction

Chronic myelogenous leukemia (CML) and Philadelphia (Ph)-positive acute lymphocytic leukemia (ALL) are caused by the unregulated activity of chimeric Bcr-Abl protein in white blood cells [1]. Gleevec® (Imatinib mesylate) is a first generation BCR-ABL kinase inhibitor that competitively inhibits binding of ATP to the kinase and inhibits the phosphorylation of cellular targets [2]. Treatment of CML patients with Gleevec was shown to be highly effective in clinical studies [3-5]. However, several patients showed resistance to Gleevec or experienced a relapse after initial success with the drug [6, 7]. Approximately 50% of those patients carry resistance-associated point mutations in the ATP-binding pocket of *BCR-ABL* [2, 8, 9]. In the remaining 50% of Gleevec-resistant patients, several mechanisms of resistance have been described, including amplification or mutation of the BCR-ABL gene and active efflux of drug from the resistant cells by ATP-binding cassette (ABC) drug transporters [10-13].

Tasigna® (nilotinib, AMN107; marketed by Novartis) is a new, orally active tyrosine kinase inhibitor (TKI) with a higher binding affinityand selectivity for BCR-ABL kinase than Gleevec [14]. Tasigna is 20 to 50 times more potent than Gleevec in Gleevec-sensitive CML cell lines and 3 to 7 times more effective in Gleevec-resistant cell lines [14].

TKIs, including Gleevec and Tasigna, have recently been found to modulate drug resistance mediated by ABC drug transporters in *in vitro* and *in vivo* studies [15-17]. Although these TKIs were developed to interact specifically at the ATP-binding sites of the kinases, we showed earlier that Gleevec interacts with both Pgp and ABCG2 at the transport-substrate site(s) and not at the ATP-binding site(s) of ABC drug transporters [18]. Existing literature does not provide definitive data on the effectiveness of TKIs (specifically Tasigna, which is used to treat imatinib-resistant CML patients) in ABC-drug-transporter-expressing CML cells [18]. Therefore, we sought to address this aspect of TKI-ABC drug transporter interactions using a fluorescent and a radiolabeled derivative of this drug. We synthesized a fluorescent (BODIPY® FL) derivative of Tasigna and this study highlights the interaction of this fluorescent derivative (BODIPY® FL Tasigna) with Pgp and ABCG2 using both cell-based *in vitro* and *ex vivo* assays. In addition, we studied the transport of a radiolabeled [^{3}H] derivative of Tasigna in polarized LLC-PK cells expressing Pgp. The results from these two derivatives of Tasigna demonstrate that Tasigna is transported by Pgp and ABCG2. These data may have important pharmacological and toxicological significance, as Tasigna is an orally active drug recently approved by the FDA for the treatment of CML and its safety and efficacy profile are still under investigation.

Experimental Section

Chemicals

Mitoxantrone, MTT dye, rhodamine 123 and all other chemicals were purchased from Sigma (St. Louis, MO). [^{125}I]-iodoarylazidoprazosin (IAAP) (2200 Ci/mmole) was from Perkin Elmer Life Sciences (Wellesley, MA). XR9576 and PSC833 were a kind gift from Xenova (UK) and Novartis (Basel, Switzerland), respectively. FTC was synthesized by Thomas McCloud, National Cancer Institute, NIH. The BODIPY® FL labeling kit and BODIPY® FL prazosin were purchased from Invitrogen Corp. (Carlsbad, CA), and [N-ε (4-nitrobenzofurazan-7-yl)-D-Lys8]-cyclosporine A (NBD-CSA) was synthesized by R. Wenger (Basel, Switzerland) [19]. [^{3}H]-Tasigna (370-740 GBq/mmol) was custom prepared by using the [^{3}H] exchange method by American Radiolabeled Chemicals, Inc. (St. Louis, MO).

Cell lines and culture conditions

pCDNA3.1-HEK, Pgp-HEK, ABCG2-HEK and K562-ABCG2 cells were kind gifts from Dr. Susan Bates (NCI, NIH) and were maintained in DMEM (with 2 mM L-glutamine and 10% FBS) with 2 mg/ml G-418. K562 and K562/i-S9 (Pgp) cells were provided by Dr. Eugene Mechetner (Oncotech Inc, Tustin, CA). K562, K562/i-S9 and K562-ABCG2 were maintained in RPMI media (with 2 mM L-glutamine and 10% FBS) [20]. LLC-PK1 control (ATCC, Manassas, VA) and LLC-PK1-*MDR*1 cells were grown in medium 199 (3% (v/v) FBS, 1% Penicillin/Streptomycin and 500μg/ml Geneticin). The expression levels of Pgp and ABCG2 in HEK and K562 cells were different, as demonstrated earlier [20-23].

Generation of LLC-PK1-*MDR*1 cell line

LLC-PK1 cells expressing human Pgp were generated by transfecting these cells with pcDNA3.1 plasmid containing human wild-type Pgp cDNA using Lipofectamine 2000 (Invitrogen, CA). After transfection, stable recombinant cells were isolated and the expression recombinant human Pgp on the cell membrane were verified by western blot analysis and Flow cytometry using Pgp specific monoclonal C219 and MRK16 antibodies, respectively and Calcein-AM accumulation assays.

Animals

Male Sprague-Dawley rats (10 weeks old, 300 g average body weight) were purchased from Charles River (Portage, MI). All animal protocols were approved by the Institutional Animal Care and Use Committee of the University of Minnesota (IACUC protocol # 0710A17842; PI: Björn Bauer) and were in accordance with AAALAC regulations and the Guides to Animal Use of the University of Minnesota and NIH animal use guidelines.

Isolation of crude membranes

Crude membranes from High-five insect cells expressing Pgp were prepared as described elsewhere [24]. The protein content was estimated using the amido black B-dye binding assay, as described previously [25].

Fluorescent drug accumulation assay by Flow Cytometry

Accumulation assays with BODIPY® FL Tasigna (0.5 μM) were performed as described previously [26]. For all samples, 10,000 events were counted and the analysis was performed with Cell Quest software (Becton-Dickinson Immunocytometry systems). The mean fluorescence intensity was calculated using the histogram stat program in Cell Quest software.

Confocal microscopy

pcDNA3.1-HEK, Pgp-HEK and ABCG2-HEK cells were grown on 12-well glass bottom chamber slides for 14-16 hr (Nalge Nunc International Corp, Naperville, IL). These cells were incubated with 0.5 μM BODIPY® FL Tasigna (in IMDM media containing 5% FBS) at 37°C for 45 min. The cells were washed twice with cold PBS and images were acquired using an oil immersion objective (100 X) in a confocal microscope (MRC-1024, Bio-Rad, Hercules, CA, USA).

ATPase and photoaffinity labeling assays

For ATPase assays, crude membrane protein (100 μg protein/ml) from High-five cells expressing Pgp and ABCG2 was incubated at 37°C with varying concentrations of Tasigna and ATP in the presence and absence of 0.3 mM sodium orthovanadate and the vanadate-

sensitive ATPase activity was determined by estimating the amount of inorganic phosphate released, as described previously [24].

Photoaffinity assays were performed by incubating crude membranes (1 mg protein/ml) from Pgp-expressing or ABCG2-expressing High-five cells with 0-20 μM of Tasigna for 10 min at 21-23°C in 50 mM Tris-HCl, pH 7.5 followed by addition of 3-6 nM [^{125}I]-IAAP (2200 Ci/mmole). The samples were crosslinked and incorporation of [^{125}I]-IAAP was determined as described previously [27].

Transport assay in rat brain capillaries

Rat brain capillaries are known to express Pgp and ABCG2 [28, 29], therefore freshly isolated capillaries from rat brains were used to monitor Pgp and ABCG2 transport function with fluorescent substrates including Bodipy-Tasigna® as previously described [30, 31]. Brain capillaries were incubated for 1 h at room temperature with either 2 μM NBD-CSA, 2 μM BODIPY® FL prazosin, or 2 μM BODIPY® FL Tasigna. For each treatment, images of 10 capillaries were acquired by confocal microscopy (Nikon C1 laser scanning confocal microscope unit mounted on a Nikon TE2000 inverted microscope, 40x oil immersion objective, numerical aperture × 1.3, 488 nm line of a Spectra Physics krypton-argon laser (model 163C) in conjunction with a 515/30nm band pass filter; Nikon Instruments Inc., Melville, NY, USA). Confocal images were analyzed by measuring the lumenal fluorescence intensity of the above compounds as described previously [30, 31].

Immnuoblotting

10^6 cells from LLC-PK1 (parental) and LLC-PK1-MDR1 (P-gp positive) cell lines were solubilized in protein extraction buffer (10mM Tris-HCl, pH8.0, 0.1% Triton X-100 (v/v), 10 mM $MgSO_4$, 2 mM $CaCl_2$ supplemented with 1% (v/v) aprotinin, 1 mM AEBSF, 2 mM DTT and 20 μg/ml micrococcal nuclease. Samples were lysed by freeze thaw following sonication in a bath sonicator. Equal amount of protein samples were separated by SDS-PAGE on 3-8% Tris-Acetate gel and transfer onto nitrocellulose membrane. The blot was blocked with 20% non-fat dry milk followed by overnight incubation with Pgp-specific C219 antibody (1:2000). Horseradish peroxidase-conjugated anti-mouse IgG was used as secondary antibody. The presence of Pgp was visualized by enhanced chemiluminescence reagents (Perkin-Elmer) according to manufacturer's protocol.

Transepithelial transport assay

LLC-PK1-MDR1 cells were seeded at a density of 2×10^6 cells/24mm well on transwell costar polycarbonate filters (0.4μm pore size, Costar, Lowell, MA). Cells were cultured for 5 days with media changed once in two days. To confirm the quality of the cell monolayers, transepithelial electrical resistance (TEER) was measured with an epithelial voltmeter (World Precision Instruments, Sarasota, FL). Cell monolayers with TEER values above 200Ω were used for assay. The transport across the cell monolayer was conducted by adding [^{3}H]-Tasigna (64 nM, 1 μCi/ml) to either the apical or basolateral side of the monolayer in the absence or presence of cyclosporine A (10 μM) or tariquidar (1 μM). Aliquots of medium (50 μl) were taken from the opposite side of the cell monolayer at 60, 120, 180 and 240 minutes, mixed with scintillation cocktail (10 ml) (Bio-Safe II) and the disintegrations per minute were measured using a Beckman Coulter LS-6500 liquid scintillation analyzer. The efflux ratio (B→A/A→B), in folds, were calculated by dividing drug efflux rate of (B→A) from (A→B) to evaluate Pgp-mediated directional efflux.

Measurement of BCR-ABL kinase activity in K562 cells

K562, K562/i-S9 and K562 ABCG2 cells were treated with 0.05-1 μM Tasigna or 10-20 μM BODIPY® FL Tasigna for 4 hr. BCR-ABL kinase activity was measured in total cell lysates by detecting the levels of P-Crkl, a BCR-ABL kinase target using P-Crkl (Tyr207) or total Crkl levels using CrkL antibodies (Cell Signaling Technology, Danvers, MA) according to the manufacturer's suggested protocol.

Synthesis of Tasigna and BODIPY® FL Tasigna

The synthesis of Tasigna was accomplished using a series of published methods [32]. The complete synthetic scheme for BODIPY® FL Tasigna is shown in Figure 3. Detailed characterization of the intermediates in the synthesis protocol and an analytical trace demonstrating the purity of BODIPY® FL Tasigna is given in the supplementary information section.

Statistical Analysis

Data are presented as mean ± SEM. A two-tailed unpaired Student's t test was used to evaluate differences between controls and treated groups; differences were considered to be statistically significant when $P < 0.05$. Sigmoidal dose-response curves and IC_{50} values were calculated using GraphPad Prism Software Version 4.01 (GraphPad Software, Inc., La Jolla, CA, USA).

Results

Tasigna inhibits the transport of substrates by Pgp-overexpressing cells

To investigate the interaction of Tasigna with Pgp, its effect on the Pgp-mediated efflux of calcein-AM was determined. Control pcDNA3.1-HEK and Pgp-expressing Pgp-HEK cells were incubated with 0.25 μM calcein-AM in the presence or absence of indicated concentrations of Tasigna or 2 μM, Tariquidar (XR9576; a Pgp-specific inhibitor) at 37°C for 10 min. The total cellular fluorescence was monitored using flow cytometry as described in the Experimental section. As shown in Figure 1a, 1-2 μM Tasigna inhibited the efflux of calcein-AM in Pgp-HEK cells, while it had no effect on the accumulation of this compound in control pCDNA3.1-HEK cells. The inhibition of calcein-AM efflux by Tasigna was comparable to 2 μM XR9576, suggesting that Tasigna was a potent inhibitor of the function of Pgp.

Tasigna interacts at the substrate binding pocket of Pgp

To understand the mechanism of interaction of Tasigna with Pgp, we determined the effect of Tasigna on Pgp ATPase activity and its ability to displace IAAP binding in photoaffinity labeling assays. Tasigna inhibited the photolabeling of Pgp with [^{125}I]-IAAP in a concentration-dependent manner with an IC_{50} value of 0.18 μM and stimulated ATP hydrolysis at very low concentrations, with only 0.19 μM required for 50% stimulation (Figure 1b and c). These results demonstrate that Tasigna interacts with the drug substrate binding site(s) on Pgp in a way similar to its interaction with drug substrate binding sites on ABCG2 reported earlier [33]. Tasigna also stimulated the ABCG2-ATPase activity in a concentration-dependent manner [see Figure 3 in reference [33]].

Tasigna inhibits Pgp and ABCG2 transport function at the blood-brain barrier

An important physiological function of Pgp and ABCG2 is to provide a pharmacological barrier for tissues present in the blood-tissue interphase such as in the blood-brain barrier. Since Tasigna inhibits the transport function of Pgp in cultured cells (Figure 1a), we then sought to determine if it was also effective in an *ex vivo* system consisting of freshly

isolated, intact rat brain capillaries, which express both Pgp and ABCG2 and are an established *ex vivo* model to study blood-brain barrier function [34-37]. Isolated brain capillaries were exposed to either 2 μM NBD-CSA (fluorescent Pgp substrate), or 2 μM BODIPY® FL prazosin (fluorescent ABCG2 substrate) for 1 h with or without Tasigna. In capillaries treated with Tasigna, lumenal fluorescence of both NBD-CSA and BODIPY® FL prazosin was reduced in a dose-dependent manner (Figure 1d and 1e middle panels). PSC833, a Pgp-specific inhibitor, and fumitremorgin C (FTC), an ABCG2-specific inhibitor, also reduced lumenal fluorescence of NBD-CSA and BODIPY® FL prazosin, respectively (Figures 1d and 1e, right panel). Quantification of steady-state lumenal fluorescence accumulation showed that Tasigna, PSC833, and FTC maximally reduced lumenal fluorescence to approximately 50% of control capillaries (Figure 1f and 1g). Note that the fluorescence remaining after inhibition of transport reflects passive diffusion and nonspecific binding of the dye to the tissue [36, 37]. The IC_{50} concentrations for Tasigna to inhibit efflux activity were 3.46 μM for Pgp and 93.2 nM for ABCG2, respectively.

Tasigna reverses resistance of Pgp-expressing cells to the anticancer drug doxorubicin

The effect of Tasigna on the cytotoxicity of other anticancer drugs is further demonstrated by the reversal of cytotoxicity assays where a non-toxic concentration of Tasigna in combination with the Pgp substrate doxorubicin was able to inhibit drug resistance mediated by Pgp in MDR1-transfected HEK cells (Table 1).

Tasigna is less effective at inhibiting BCR-ABL kinase in Pgp- and ABCG2-expressing CML cells

Since Tasigna targets the BCR-ABL kinase in CML cells, we evaluated its ability to inhibit BCR-ABL kinase activity in CML cells that overexpress Pgp and ABCG2. The BCR-ABL kinase activity was measured by monitoring the phosphorylation of Crkl (P-Crkl), a target of BCR-ABL kinase in K562 cells (a CML cell line) since this kinase is specifically expressed in this these cells. Tasigna was less effective at inhibiting the phosphorylation of Crkl in Pgp-expressing K562/i-S9 cells (Figure 2a, upper panel), and ABCG2-expressing K562-ABCG2 cells (Figure 2b, upper panel) compared to that in parental, control K562 cells. The level of total Crkl remained unchanged in these cells by treatment with Tasigna (Figure 2a and 2b, lower panels). The level of P-Crkl expression was quantitated by densitometric analysis. The IC_{50} value of Tasigna for inhibition of Crkl phosphorylation in K562 cells was 69.85 nM, while it was 329 nM for K562/i-S9 (Pgp) cells and 370 nM for K562-ABCG2 cells (Figure 2b). Tasigna was thus 4-to 5-fold less effective at inhibiting BCR-ABL kinase activity in Pgp- and ABCG2-expressing K562 cells compared to control K562 cells. A plausible reason for the reduced efficacy of Tasigna in Pgp- and ABCG2-expressing cells could be lower intracellular levels of the drug due to Pgp- and ABCG2-mediated active efflux from these cells as compared to control K562 cells.

Synthesis of BODIPY-conjugate of Tasigna

The above described results indicated that active efflux of Tasigna by Pgp and ABCG2 in CML cells can lead to its reduced efficacy. However, there was no clear evidence that Tasigna was transported by Pgp or ABCG2. In order to address this question, we synthesized a fluorescent derivative of Tasigna (Figure 3) as described in the Experimental section and evaluated it in fluorescence-based *in vitro* and *ex vivo* assays. Previously, BODIPY conjugates of anticancer agents including vinblastine, verapamil and paclitaxel have been used as tools to determine transport function of ABC drug transporters [38, 39]. The basic physicochemical properties of Tasigna and a truncated version of Bodipy-Tasigna molecule (the programs used can't deal with the multivalency of the boron in the Bodipy fluorophore so it had to be removed) are significantly similar (the Log P values of Tasigna and its fluorescent derivative are 4.95 and 3.68, respectively). Further analysis showed that

the only major difference between Tasigna and Bodipy-Tasigna is within the polar surface area which understandably goes way up for Bodipy-Tasigna. There is no clear data that suggest this should have an effect on passive membrane permeability.

BODIPY® FL Tasigna is transported by Pgp- and ABCG2-expressing K562 and HEK cells

BODIPY® FL Tasigna proved to be an effective tool to study the intracellular Tasigna levels in cells expressing Pgp and ABCG2 with both flow cytometry (Figure 4a) and confocal microscopy (Figure 4b). Since K562 cells do not grow as a monoloayer, but remain in suspension, they could not be analyzed by confocal microscopy. The confocal images were therefore acquired with only HEK cells. K562, K562/i-S9 (Pgp), and K562-ABCG2 (Figure 4a) or pcDNA3.1-HEK, Pgp-HEK, and ABCG2-HEK (Figure 4b) cells were incubated with 0.25 μM BODIPY® FL Tasigna in the presence or absence of different Pgp/ABCG2 inhibitors as described in the Experimental section. While control cells showed high levels of accumulation of BODIPY® FL Tasigna, the Pgp- and ABCG2-expressing cells had low levels of accumulation (Figure 4a and b). Addition of 2 μM Tariquidar (XR 9576, Pgp inhibitor) or 10 μM FTC (ABCG2 inhibitor) completely blocked active efflux of BODIPY® FL Tasigna, thereby increasing total cellular accumulation of the compound (Figure 4b). These results demonstrate that the total intracellular levels of the BODIPY® FL Tasigna in Pgp- and ABCG2-expressing cells are lower than in cells that do not express these transporters, indicating that it is actively pumped out of these cells and that BODIPY® FL Tasigna is a transport substrate for both Pgp and ABCG2. These results substantiate the results shown in Figure 2 suggesting that Pgp- and ABCG2-mediated cellular efflux of Tasigna could be responsible for the decreased intracellular Tasigna levels and its reduced effectiveness at inhibiting BCR-ABL kinase in Pgp- and ABCG2-expressing K562 cells. It should be noted that the difference in total intracellular levels of BODIPY® FL Tasigna in K562 cells (Figure 4a) were modest compared to the HEK cells (Figure 4b). This may be attributed to differences in the expression levels of Pgp and ABCG2 in K562 cells compared to HEK cells (see ref. 41-44).

BODIPY® FL Tasigna inhibits BCR-ABL kinase activity in CML cells

To demonstrate that the properties of Tasigna are not drastically altered in conjugated BODIPY® FL Tasigna, we characterized its activity in inhibiting BCR-ABL kinase activity. Figure 5a (upper panel) shows that 10-20 μM BODIPY® FL Tasigna inhibited the phosphorylation of Crkl in K562 cells, while total Crkl levels remained unchanged (lower panel) suggesting specific inhibition of phosphorlyation of Crkl. These data suggested that conjugation of Tasigna with the BODIPY group did not qualitatively alter the BCR-ABL kinase inhibitory potential of the parent drug Tasigna. It should be noted that BODIPY® FL Tasigna was less potent than Tasigna in inhibiting BCR-ABL kinase (a potential consequence of the structural alteration of the molecule and/or cytosolic exposure of the conjugate relative to free drug).

BODIPY® FL Tasigna is effluxed at the blood-brain barrier and it interacts at the substrate-binding pocket of Pgp and ABCG2

To further confirm that BODIPY® FL Tasigna can be used as an surrogate tool to monitor Tasigna's interactions with ABC drug transporters under *ex vivo* conditions, freshly isolated rat brain capillaries were incubated with BODIPY® FL Tasigna for 1 h. As shown in Figure 5b and c, BODIPY® FL Tasigna was actively effluxed into the lumen of brain capillaries (Figure 5b and c). This could be inhibited by Tasigna and PSC833 or FTC, specific inhibitors of Pgp and ABCG2, respectively. In addition, BODIPY® FL Tasigna also inhibited the binding of ^{125}I-IAAP to Pgp and ABCG2 (Figure 5d), indicating that similar to Tasigna, fluorescent Tasigna also interacts at the substrate binding site(s) on Pgp and ABCG2. These results clearly showed that BODIPY® FL Tasigna is pumped out by Pgp

and ABCG2 present at the blood-brain barrier and that this compound interacts with the substrate binding pocket in a manner similar to other typical substrates of these transporters. Consistent with these results, BODIPY® FL Tasigna also stimulated the ATPase activity of Pgp and ABCG2, respectively (data not shown). It should be noted that the IC_{50} for inhibition of Crkl activity, inhibition of ^{125}I-IAAP binding and the concentration required for 50% stimulation of ATP hydrolysis for BODIPY® FL Tasigna was 5- to 7-fold higher than that for Tasigna. The observed lower activity may be due to the larger size of BODIPY® FL Tasigna (mol. wt. 1108.49) compared to parent compound (mol. wt. 530.18) and/or the altered cellular exposure to the conjugate. BODIPY® FL Tasigna may therefore be especially useful in studies of the interactions of tyrosine kinase inhibitors with Pgp, as this and other TKIs are known to interact with ABC transporters with a higher affinity, making it difficult to observe the TKI transport differences in intact cell assays.

[^{3}H]-Tasigna is transported by Pgp—To confirm further that Tasigna is a transport substrate of Pgp, we used polarized LLC-PK1 cells expressing Pgp (Figure 6a) and evaluated ability of these cells to efflux [^{3}H]-Tasigna in transepithelial transport assay (Figure 6b). Cells were incubated with [^{3}H]-Tasigna (64 nM) and drug transport across the cell monolayer was measured for 4 hrs. [^{3}H]-Tasigna transport from the basolateral to the apical compartment (B→A) was significantly higher than transport from the apical to the basolateral compartment (A→B) and a time-dependent linear increase in drug transport across the cell monolayer was observed (Figure 6b). The fold difference in B→A versus A→B [^{3}H]-Tasigna transport at 180 minutes was 5.64 ± 0.44 (Figure 6c). Inhibition of Pgp function with cyclosporine A (10 μM) or tariquidar (1 μM) significantly reduced the B→A transport rate, indicating that the observed transport across polarized LLCPK1 cells was Pgp-specific. Taken together, the results with [^{3}H]-Tasigna and BODIPY® FL Tasigna clearly demonstrate that Tasigna is a transport substrate of Pgp.

Discussion

Expression of the ABC drug transporters Pgp and ABCG2 has been associated with the development of drug resistance to first generation BCR-ABL kinase inhibitors such as Gleevec [12,40-42].Tasigna, a second generation BCR-ABL kinase inhibitor has been developed as more potent and specific inhibitor that also inhibits the kinase activity of mutant Gleevec-resistant BCR-ABL kinases. Several conflicting reports have been published about the above kinase inhibitors being substrates of ABC drug transporters. While some groups have shown that resistance to Gleevec is due to its low intracellular accumulation [33, 43, 44], other reports have suggested that the resistance is not dependent on drug efflux by ABC drug transporters [45, 46]. In the case of Tasigna, it has also been shown that Tasigna interacts with ABCG2 with a very high affinity, is a substrate of this drug transporter, and reverses drug resistance mediated by Pgp and ABCG2 [17, 33], while others reported that cellular accumulation of Tasigna in cell lines and primary CD34(+) CML cells is not mediated by active uptake or efflux by major drug transporters and expression of Pgp may not be enough to confer drug resistance to Tasigna [15, 47]. However, the nature of the interaction of Tasigna with Pgp is not very well understood. Moreover, the effectiveness of Tasigna in inhibiting BCR-ABL kinase activity in Pgp- and ABCG2- expressing leukemic cells has also not been studied mechanistically.

The data from this study indicate that Tasigna inhibits Pgp activity by interacting with the substrate binding pocket of Pgp, similar to results obtained previously with ABCG2 (Figure 1 and [33]). This inhibition of Pgp and ABCG2 function at low micromolar and nanomolar concentrations, respectively, can influence the toxicity or bioavailability of other drugs or metabolites in humans that are substrates of ABC drug transporters. Systemic concentrations of Tasigna after administration of the recommended twice daily dose of 400 mg ranges from

1.7 to 3.6 μM [48]. Therefore, the above experimental concentrations of Tasigna can be achieved systemically in CML patients treated with Tasigna, which may further inhibit Pgp physiologically, representing another cellular target for Tasigna that may arise in a secondary phenotypic outcome. Direct evidence for this is presented in our experiments with rat brain capillaries, where Tasigna inhibits Pgp and ABCG2 function resulting in decreased efflux activity of these transporters at the blood-brain barrier.

A fluorescent derivative of Tasigna was synthesized to study its direct interaction with ABC drug transporters (Figure 3 and supplementary information). We showed for the first time that the total intracellular levels of BODIPY® FL Tasigna in Pgp- and ABCG2-expressing cells were lower than in cells that do not express these transporters, indicating that it is actively pumped out of these cells (Figure 4). This efflux of BODIPY® FL Tasigna was inhibited by specific inhibitors of Pgp and ABCG2 in both *in vitro* and *ex vivo* assays (Figures 4 and 5). This fluorescent derivative also inhibited the BCR-ABL kinase activity although with a lower efficiency that could be attributed to the structural alteration of the molecule, possibly resulting in decreased affinity to its target (Figure 5).

[^{3}H]-labeled Tasigna was also synthesized to test whether it is a transport substrate for Pgp. The polarized LLC-PK1 cells expressing Pgp were used to determine [^{3}H] Tasigna transport. The data clearly demonstrated a net active transport of [^{3}H]-Tasigna from the basal to apical side of the polarized LLC-PK1 cells expressing Pgp and Pgp inhibitors significantly blocked the directional flux of radiolabeled Tasigna (Figure 6). These data validate the results obtained with BODIPY® FL Tasigna. However, Hegedus *et al* [15], based on an HPLC-MS assay, reported that there was no significant difference in the amount of intracellular Tasigna in control and Pgp-expressing K562 cells (non polarized cells). At present, we do not know the reason for failure to observe transport in non-polarized cells, but most likely it could be the result of high background due to non-specific binding of Tasigna to cells (also mentioned by these authors).

Our results with both the fluorescent derivative and [^{3}H]-Tasigna collectively show that this TKI is transported by Pgp and ABCG2. Based on these data, we conclude that Tasigna is a less potent inhibitor of BCR-ABL kinase activity in Pgp- or ABCG2-expressing drug-resistant CML cells compared to sensitive control CML cells because it is transported by Pgp and ABCG2, resulting in reduced intracellular accumulation. This is an important finding given the clinical application of Tasigna, which is administered to drug-resistant CML and ALL patients. This reduced effectiveness becomes more important in a scenario where the expression of ABC transporters is increased in patients who have been treated with a drug that is a transporter substrate and the incidence of secondary resistance increases because the drug becomes ineffective due to active efflux by these transporters. In fact, despite the initial clinical effectiveness of Tasigna in CML resistant patients, lack of response to Tasigna therapy and development of resistance have also been reported [14, 49].

A non-toxic concentration of Tasigna in combination with the Pgp substrate doxorubicin was able to inhibit drug resistance mediated by Pgp in MDR1-transfected HEK cells (Table 1). These observations could have dual implications in the clinic. Administering Tasigna with drugs that are substrates of Pgp could result in increased systemic concentrations of these drugs. Alternatively, administering Tasigna with drugs that inhibit Pgp function could lead to increased Tasigna toxicity. The FDA summary review for approval of Tasigna reflects these two possibilities, stating that treatment with Tasigna may result in increased toxicity or drug/drug interactions if administered with drugs which are either Pgp substrates or inhibitors (http://www.fda.gov/cder/foi/nda/2007/022068s000_SumR.pdf). Increased oral bioavailability or antitumor response of anticancer drugs in combination with other TKIs

such as Gleevec, Gefitinib or Lapatinib has already been shown by a number of studies [50-53].

In conclusion, our findings indicate that interaction of Tasigna with Pgp and ABCG2 may be an important factor in the treatment of CML and AML patients, as efflux of Tasigna by Pgp and ABCG2 may result in resistance to this drug. Moreover, interaction with Pgp and ABCG2 can modify the pharmacokinetic and toxicity profile of Tasigna in *vivo*. Additional studies to specifically investigate the interaction of Tasigna with ABC transporters may be warranted to determine its efficacy in the treatment of Gleevec-resistant CML and ALL. In addition, BODIPY FL® Tasigna may represent an important tool for researchers to follow the efficacy, pharmacokinetics, and toxicity of Tasigna in preclinical and clinical models. A similar approach may be used to study whether a given TKI is transported by Pgp or ABCG2. It could also be adapted for use in *in vivo* imaging studies to assess the accumulation of xenobiotics in the brain that are transported by Pgp or ABCG2. To our knowledge, this is the first study that not only demonstrates direct transport of Tasigna by Pgp in transepithelial monolayer assays but also reports synthesis and characterization of a fluorescent derivative of a TKI that is not only active in inhibiting the target kinase but can also be used to study its interaction with other proteins such as ABC drug transporters in cancer cells.

Supplementary Material

Refer to Web version on PubMed Central for supplementary material.

Acknowledgments

This work was supported by the Intramural Research Program of the NIH, National Cancer Institute, Center for Cancer Research. We thank Dr. Krishnamachary Nandigama for providing Pgp-expressing High-five insect cell crude membranes, Anne Ramsey for help in kinase assays, and George Leiman for editorial assistance.

Abbreviations

ABC	ATP binding Cassette
BCR-ABL	breakpoint cluster region-abelson
FTC	Fumitremorgin C
IAAP	Iodoarylazidoprazosin
Pgp	P-glycoprotein
TKI	tyrosine kinase inhibitor

References

1. Savona M, Talpaz M. Getting to the stem of chronic myeloid leukaemia. Nat. Rev. Cancer. 2008; (5):8, 341–350.
2. Schindler T, Bornmann W, Pellicena P, Miller WT, Clarkson B, Kuriyan J. Structural Mechanism for STI-571 Inhibition of Abelson Tyrosine Kinase. Science. 2000; 289(5486):1938–1942. [PubMed: 10988075]
3. Druker BJ, Talpaz M, Resta DJ, Peng B, Buchdunger E, Ford JM, Lydon NB, Kantarjian H, Capdeville R, Ohno-Jones S, Sawyers CL. Efficacy and Safety of a Specific Inhibitor of the BCR-ABL Tyrosine Kinase in Chronic Myeloid Leukemia. N. Engl. J. Med. 2001; 344(14):1031–1037. [PubMed: 11287972]
4. Kantarjian H, Sawyers C, Hochhaus A, Guilhot F, Schiffer C, Gambacorti-Passerini C, Niederwieser D, Resta D, Capdeville R, Zoellner U, Talpaz M, Druker B, the International STI571

CML Study Group. Hematologic and Cytogenetic Responses to Imatinib Mesylate in Chronic Myelogenous Leukemia. N. Engl. J. Med. 2002; 346(9):645–652. [PubMed: 11870241]

5. O'Brien SG, Guilhot F, Larson RA, Gathmann I, Baccarani M, Cervantes F, Cornelissen JJ, Fischer T, Hochhaus A, Hughes T, Lechner K, Nielsen JL, Rousselot P, Reiffers J, Saglio G, Shepherd J, Simonsson B, Gratwohl A, Goldman JM, Kantarjian H, Taylor K, Verhoef G, Bolton AE, Capdeville R, Druker BJ, the IRIS Investigators. Imatinib Compared with Interferon and Low-Dose Cytarabine for Newly Diagnosed Chronic-Phase Chronic Myeloid Leukemia. N. Engl. J. Med. 2003; 348(11):994–1004. [PubMed: 12637609]
6. Gorre ME, Mohammed M, Ellwood K, Hsu N, Paquette R, Rao PN, Sawyers CL. Clinical Resistance to STI-571 Cancer Therapy Caused by BCR-ABL Gene Mutation or Amplification. Science. 2001; 293(5531):876–880. [PubMed: 11423618]
7. Druker BJ. STI571 (Gleevec(TM)) as a paradigm for cancer therapy. Trends Mol. Med. 2002; 8(4):S14–S18. [PubMed: 11927282]
8. Shah NP, Nicoll JM, Nagar B, Gorre ME, Paquette RL, Kuriyan J, Sawyers CL. Multiple BCR-ABL kinase domain mutations confer polyclonal resistance to the tyrosine kinase inhibitor imatinib (STI571) in chronic phase and blast crisis chronic myeloid leukemia. Cancer Cell. 2002; 2(2):117–125. [PubMed: 12204532]
9. Azam M, Seeliger MA, Gray NS, Kuriyan J, Daley GQ. Activation of tyrosine kinases by mutation of the gatekeeper threonine. Nat Struct Mol Biol. 2008; 15(10):1109–1118. [PubMed: 18794843]
10. Mahon FX, Deininger MWN, Schultheis B, Chabrol J, Reiffers J, Goldman JM, Melo JV. Selection and characterization of BCR-ABL positive cell lines with differential sensitivity to the tyrosine kinase inhibitor STI571: diverse mechanisms of resistance. Blood. 2000; 96(3):1070–1079. [PubMed: 10910924]
11. le Coutre P, Tassi E, Varella-Garcia M, Barni R, Mologni L, Cabrita G, Marchesi E, Supino R, Gambacorti-Passerini C. Induction of resistance to the Abelson inhibitor STI571 in human leukemic cells through gene amplification. Blood. 2000; 95(5):1758–1766. [PubMed: 10688835]
12. Mahon F-X, Belloc F, Lagarde V, Chollet C, Moreau-Gaudry F, Reiffers J, Goldman JM, Melo JV. MDR1 gene overexpression confers resistance to imatinib mesylate in leukemia cell line models. Blood. 2003; 101(6):2368–2373. [PubMed: 12609962]
13. Thomas J, Wang L, Clark RE, Pirmohamed M. Active transport of imatinib into and out of cells: implications for drug resistance. Blood. 2004; 104(12):3739–3745. [PubMed: 15315971]
14. Kantarjian H, Giles F, Wunderle L, Bhalla K, O'Brien S, Wassmann B, Tanaka C, Manley P, Rae P, Mietlowski W, Bochinski K, Hochhaus A, Griffin JD, Hoelzer D, Albitar M, Dugan M, Cortes J, Alland L, Ottmann OG. Nilotinib in Imatinib-Resistant CML and Philadelphia Chromosome-Positive ALL. N. Engl. J. Med. 2006; 354(24):2542–2551. [PubMed: 16775235]
15. Hegedus C, Ozvegy-Laczka C, Apati A, Magocsi M, Nemet K, Orfi L, Keri G, Katona M, Takats Z, Varadi A, Szakacs G, Sarkadi B. Interaction of nilotinib, dasatinib and bosutinib with ABCB1 and ABCG2: implications for altered anti-cancer effects and pharmacological properties. Br. J. Pharmacol. 2009; 158(4):1153–1164. [PubMed: 19785662]
16. Ozvegy-Laczka C, Heged""s T, Varady G, Ujhelly O, Schuetz JD, Varadi A, Keri G, Orfi L, Nemet K, Sarkadi B. High-Affinity Interaction of Tyrosine Kinase Inhibitors with the ABCG2 Multidrug Transporter. Mol. Pharmacol. 2004; 65(6):1485–1495. [PubMed: 15155841]
17. Tiwari AK, Sodani K, Wang S-R, Kuang Y-H, Ashby Jr CR, Chen X, Chen Z-S. Nilotinib (AMN107, Tasigna®) reverses multidrug resistance by inhibiting the activity of the ABCB1/Pgp and ABCG2/BCRP/MXR transporters. Biochem. Pharmacol. 2009; 78(2):153–161. [PubMed: 19427995]
18. Shukla S, Sauna ZE, Ambudkar SV. Evidence for the interaction of imatinib at the transport-substrate site(s) of the multidrug-resistance-linked ABC drug transporters ABCB1 (P-glycoprotein) and ABCG2. Leukemia. 2008; 22(2):445–447. [PubMed: 17690695]
19. Schramm U, Fricker G, Wenger R, Miller DS. P-glycoprotein-mediated secretion of a fluorescent cyclosporin analogue by teleost renal proximal tubules. Am. J. Physiol. Renal Physiol. 1995; 268(1):F46–52.

20. Mechetner EB, Schott B, Morse BS, Stein WD, Druley T, Davis KA, Tsuruo T, Roninson IB. P-glycoprotein function involves conformational transitions detectable by differential immunoreactivity. Proc. Natl. Acad. Sci. U. S. A. 1997; 94(24):12908–12913. [PubMed: 9371774]
21. Shafran A, Ifergan I, Bram E, Jansen G, Kathmann I, Peters GJ, Robey RW, Bates SE, Assaraf YG. ABCG2 harboring the Gly482 mutation confers high-level resistance to various hydrophilic antifolates. Cancer Res. 2005; 65(18):8414–8422. [PubMed: 16166320]
22. Robey RW, Honjo Y, Morisaki K, Nadjem TA, Runge S, Risbood M, Poruchynsky MS, Bates SE. Mutations at amino-acid 482 in the ABCG2 gene affect substrate and antagonist specificity. Br. J. Cancer. 2003; 89(10):1971–1978. [PubMed: 14612912]
23. Hiwase DK, Saunders V, Hewett D, Frede A, Zrim S, Dang P, Eadie L, To LB, Melo J, Kumar S, Hughes TP, White DL. Dasatinib cellular uptake and efflux in chronic myeloid leukemia cells: therapeutic implications. Clin. Cancer Res. 2008; 14(12):3881–3888. [PubMed: 18559609]
24. Ambudkar SV. Drug-stimulatable ATPase activity in crude membranes of human MDR1-transfected mammalian cells. Methods Enzymol. 1998; 292:504–514. [PubMed: 9711578]
25. Schaffner W, Weissmann C. A rapid, sensitive, and specific method for the determination of protein in dilute solution. Anal. Biochem. 1973; 56(2):502–514. [PubMed: 4128882]
26. Limtrakul P, Chearwae W, Shukla S, Phisalphong C, Ambudkar S. Modulation of function of three ABC drug transporters, P-glycoprotein (ABCB1), mitoxantrone resistance protein (ABCG2) and multidrug resistance protein 1 (ABCC1) by tetrahydrocurcumin, a major metabolite of curcumin. Mol. Cell. Biochem. 2007; 296(1):85–95. [PubMed: 16960658]
27. Shukla S, Wu C-P, Nandigama K, Ambudkar SV. The naphthoquinones, vitamin K3 and its structural analogue plumbagin, are substrates of the multidrug resistance linked ATP binding cassette drug transporter ABCG2. Mol. Cancer Ther. 2007; 6(12):3279–3286. [PubMed: 18065489]
28. Fellner S, Bauer B, Miller DS, Schaffrik M, Fankhanel M, Spruss T, Bernhardt G, Graeff C, Farber L, Gschaidmeier H, Buschauer A, Fricker G. Transport of paclitaxel (Taxol) across the blood-brain barrier in vitro and in vivo. J. Clin. Invest. 2002; 110(9):1309–1318. [PubMed: 12417570]
29. Hori S, Ohtsuki S, Tachikawa M, Kimura N, Kondo T, Watanabe M, Nakashima E, Terasaki T. Functional expression of rat ABCG2 on the luminal side of brain capillaries and its enhancement by astrocyte-derived soluble factor(s). J. Neurochem. 2004; 90(3):526–536. [PubMed: 15255930]
30. Hartz AMS, Bauer B, Block ML, Hong J-S, Miller DS. Diesel exhaust particles induce oxidative stress, proinflammatory signaling, and P-glycoprotein up-regulation at the blood-brain barrier. FASEB J. 2008; 22(8):2723–2733. [PubMed: 18474546]
31. Hartz AM, Bauer B, Fricker G, Miller DS. Rapid regulation of P-glycoprotein at the blood-brain barrier by endothelin-1. Mol. Pharmacol. 2004; 66(3):387–94. [PubMed: 15322229]
32. Wei-Sheng H, William CS. An Efficient Synthesis of Nilotinib (AMN107). Synthesis. 2007; 14:2121–2124.
33. Brendel C, Scharenberg C, Dohse M, Robey RW, Bates SE, Shukla S, Ambudkar SV, Wang Y, Wennemuth G, Burchert A, Boudriot U, Neubauer A. Imatinib mesylate and nilotinib (AMN107) exhibit high-affinity interaction with ABCG2 on primitive hematopoietic stem cells. Leukemia. 2007; 21(6):1267–1275. [PubMed: 17519960]
34. Zhang W, Mojsilovic-Petrovic J, Andrade MF, Zhang H, Ball M, Stanimirovic DB. The expression and functional characterization of ABCG2 in brain endothelial cells and vessels. FASEB J. 2003; 17(14):2085–2087. [PubMed: 12958161]
35. Eisenblatter T, Galla HJ. A new multidrug resistance protein at the blood-brain barrier. Biochem. Biophys. Res. Commun. 2002; 293(4):1273–1278. [PubMed: 12054514]
36. Bauer B, Hartz AM, Pekcec A, Toellner K, Miller DS, Potschka H. Seizure-induced up-regulation of P-glycoprotein at the blood-brain barrier through glutamate and cyclooxygenase-2 signaling. Mol. Pharmacol. 2008; 73(5):1444–1453. [PubMed: 18094072]
37. Miller DS, Bauer B, Hartz AMS. Modulation of P-Glycoprotein at the Blood-Brain Barrier: Opportunities to Improve Central Nervous System Pharmacotherapy. Pharmacol. Rev. 2008; 60(2):196–209. [PubMed: 18560012]

38. Gribar JJ, Ramachandra M, Hrycyna CA, Dey S, Ambudkar SV. Functional Characterization of Glycosylation-Deficient Human P-Glycoprotein Using A Vaccinia Virus Expression System. J. Membr. Biol. 2000; 173(3):203–214. [PubMed: 10667916]
39. Litman T, Brangi M, Hudson E, Fetsch P, Abati A, Ross DD, Miyake K, Resau JH, Bates SE. The multidrug-resistant phenotype associated with overexpression of the new ABC half-transporter, MXR (ABCG2). J. Cell Sci. 2000; 113(Pt 11):2011–2021. [PubMed: 10806112]
40. Burger H, van Tol H, Brok M, Wiemer EA, de Bruijn EA, Guetens G, de Boeck G, Sparreboom A, Verweij J, Nooter K. Chronic imatinib mesylate exposure leads to reduced intracellular drug accumulation by induction of the ABCG2 (BCRP) and ABCB1 (MDR1) drug transport pumps. Cancer Biol. Ther. 2005; 4(7):747–752. [PubMed: 15970668]
41. Hamada A, Miyano H, Watanabe H, Saito H. Interaction of imatinib mesilate with human P-glycoprotein. J. Pharmacol. Exp. Ther. 2003; 307(2):824–828. [PubMed: 12975485]
42. Prenen H, Guetens G, van Oosterom AT, De Boeck G, Highley MS, De Bruijn E. Measurement of Sediment (MESED) and LC-MS-MS for Cellular Kinetics Studies of STI-571(Imatinib, Gleevec® , Glivec®) in Cells with Different Pgp- 170 Expression Curr. Anal. Chem. 2005; 1(2): 121–127.
43. Widmer N, Rumpold H, Untergasser G, Fayet A, Buclin T, Decosterd LA. Resistance reversal by RNAi silencing of MDR1 in CML cells associated with increase in imatinib intracellular levels. Leukemia. 2007; 21(7):1561–1562. [PubMed: 17429432]
44. Illmer T, Schaich M, Platzbecker U, Freiberg-Richter J, Oelschlagel U, von Bonin M, Pursche S, Bergemann T, Ehninger G, Schleyer E. P-glycoprotein-mediated drug efflux is a resistance mechanism of chronic myelogenous leukemia cells to treatment with imatinib mesylate. Leukemia. 2004; 18(3):401–408. [PubMed: 14724652]
45. Ferrao PT, Frost MJ, Siah SP, Ashman LK. Overexpression of P-glycoprotein in K562 cells does not confer resistance to the growth inhibitory effects of imatinib (STI571) in vitro. Blood. 2003; 102(13):4499–503. [PubMed: 12881321]
46. Zong Y, Zhou S, Sorrentino BP. Loss of P-glycoprotein expression in hematopoietic stem cells does not improve responses to imatinib in a murine model of chronic myelogenous leukemia. Leukemia. 2005; 19(9):1590–1596. [PubMed: 16001089]
47. Davies A, Jordanides NE, Giannoudis A, Lucas CM, Hatziieremia S, Harris RJ, Jorgensen HG, Holyoake TL, Pirmohamed M, Clark RE, Mountford JC. Nilotinib concentration in cell lines and primary CD34+ chronic myeloid leukemia cells is not mediated by active uptake or efflux by major drug transporters. Leukemia. 2009; 23(11):1999–2006. [PubMed: 19710702]
48. Jabbour E, El Ahdab S, Cortes J, Kantarjian H. Nilotinib: a novel Bcr-Abl tyrosine kinase inhibitor for the treatment of leukemias. Expert Opin. Investig. Drugs. 2008; 17(7):1127–1136.
49. von Bubnoff N, Manley PW, Mestan J, Sanger J, Peschel C, Duyster J. Bcr-Abl resistance screening predicts a limited spectrum of point mutations to be associated with clinical resistance to the Abl kinase inhibitor nilotinib (AMN107). Blood. 2006; 108(4):1328–1333. [PubMed: 16614241]
50. Breedveld P, Pluim D, Cipriani G, Wielinga P, van Tellingen O, Schinkel AH, Schellens JH. The effect of Bcrp1 (Abcg2) on the in vivo pharmacokinetics and brain penetration of imatinib mesylate (Gleevec): implications for the use of breast cancer resistance protein and P-glycoprotein inhibitors to enable the brain penetration of imatinib in patients. Cancer Res. 2005; 65(7):2577–2582. [PubMed: 15805252]
51. Stewart CF, Leggas M, Schuetz JD, Panetta JC, Cheshire PJ, Peterson J, Daw N, Jenkins Iii JJ, Gilbertson R, Germain GS, Harwood FC, Houghton PJ. Gefitinib enhances the antitumor activity and oral bioavailability of irinotecan in mice. Cancer Res. 2004; 64(20):7491–7499. [PubMed: 15492275]
52. Leggas M, Panetta JC, Zhuang Y, Schuetz JD, Johnston B, Bai F, Sorrentino B, Zhou S, Houghton PJ, Stewart CF. Gefitinib modulates the function of multiple ATP-binding cassette transporters in vivo. Cancer Res. 2006; 66(9):4802–4807. [PubMed: 16651435]
53. Dai, C.-l.; Tiwari, AK.; Wu, C-P.; Su, X.-d.; Wang, S-R.; Liu, D.-g.; Ashby, CR., Jr.; Huang, Y.; Robey, RW.; Liang, Y.-j.; Chen, L.-m.; Shi, C-J.; Ambudkar, SV.; Chen, Z-S.; Fu, L.-w. Lapatinib (Tykerb, GW572016) Reverses Multidrug Resistance in Cancer Cells by Inhibiting the Activity of

ATP-Binding Cassette Subfamily B Member 1 and G Member 2. Cancer Res. 2008; 68(19):7905–7914. [PubMed: 18829547]

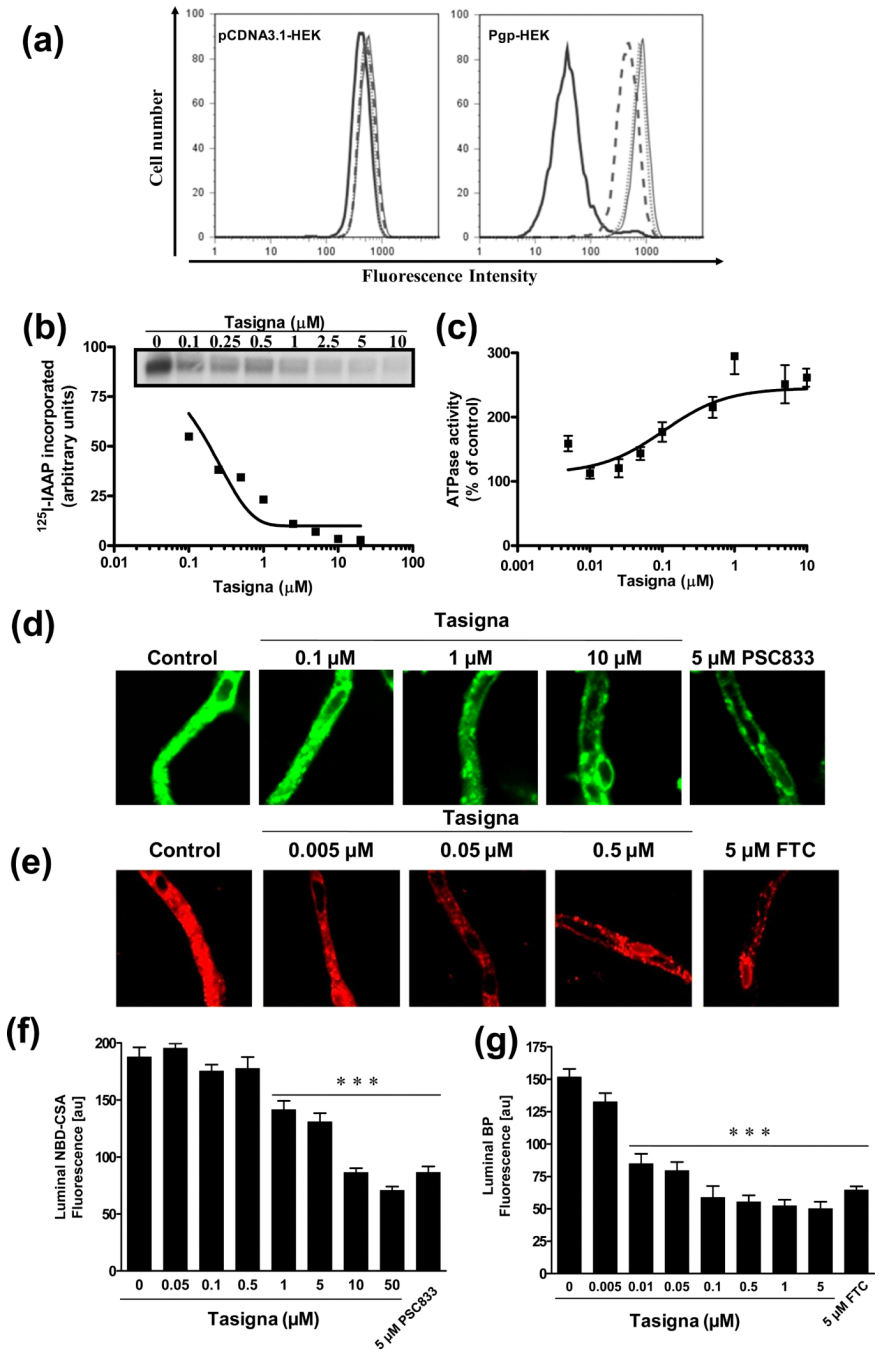

Figure 1. Tasigna inhibits Pgp-mediated efflux of calcein-AM and photoaffinity labeling of Pgp with ^{125}I-IAAP and stimulates Pgp-mediated ATP hydrolysis

(a) pCDNA3.1-HEK and Pgp-HEK cells were incubated with 0.25 μM of calcein-AM for 10 min at 37°C in the dark, in the absence (black bold) or presence of 1 μM Tasigna (dashed line), 2 μM Tasigna (dotted line) or 2 μM Pgp specific inhibitor, XR9576 (thin line). The cells were then washed and subsequently analyzed by flow cytometer as described in the Experimental section. Representative histograms from one of three independent histograms are shown. **(b)** Crude membranes from High-five cells expressing Pgp were incubated with 0-10 μM Tasigna for 5 min at 21-23°C in 50 mM Tris-HCl, pH 7.5. 3-6 nM [^{125}I]-IAAP (2200 Ci/mmole) was added and incubated for an additional 5 min under subdued light. The

samples were then illuminated with a UV lamp (365 nm) for 10 min and were processed as described in the Experimental section. The incorporation of [^{125}I]-IAAP (from autoradiogram, Y-axis) into the Pgp band was quantified by estimating the radioactivity of this band and plotted as a concentration of Tasigna (X-axis). A representative autoradiogram from one experiment is shown (inset) and similar results were obtained in two additional experiments. **(c)** Crude membrane protein from High-five cells expressing Pgp was incubated at 37°C with 0-10 μM Tasigna in the presence or absence of 0.3 mM sodium orthovanadate in an ATPase assay buffer for 10 min. The amount of inorganic phosphate released after incubation with 5 mM ATP for 20 min and the vanadate-sensitive ATPase activity was determined as described in the Experimental section. The average from three experiments is shown here and the error bars represent SE. (d, e) Tasigna inhibits Pgp and ABCG2 function in rat brain capillaries. Rat brain capillaries were incubated for 1 h at room temperature in the presence or absence of indicated concentrations of Tasigna or indicated inhibitors with (d) 2 μM NBD-CSA, a fluorescent cyclosporine A, which is a Pgp substrate or (e) 2 μM BODIPY® FL prazosin, a fluorescent ABCG2 substrate. Confocal images of 10 capillaries were acquired by confocal microscopy using a 40X oil immersion objective as described in the Experimental section. **(f, g)** Concentration-dependent decrease of lumenal NBD-CSA (f, Y-axis) or BODIPY® FL prazosin (g, Y-axis) plotted as a function of concentration of Tasigna (X-axis). Each data point represents the lumenal NBD-CSA or BODIPY® FL prazosin fluorescence mean value from 10 capillaries (pooled capillary tissue from 10 rats of a single preparation); variability is given by SEM bars. Units are arbitrary fluorescence units (au). Statistical comparison: ***, significantly lower than control capillaries, $P < 0.001$.

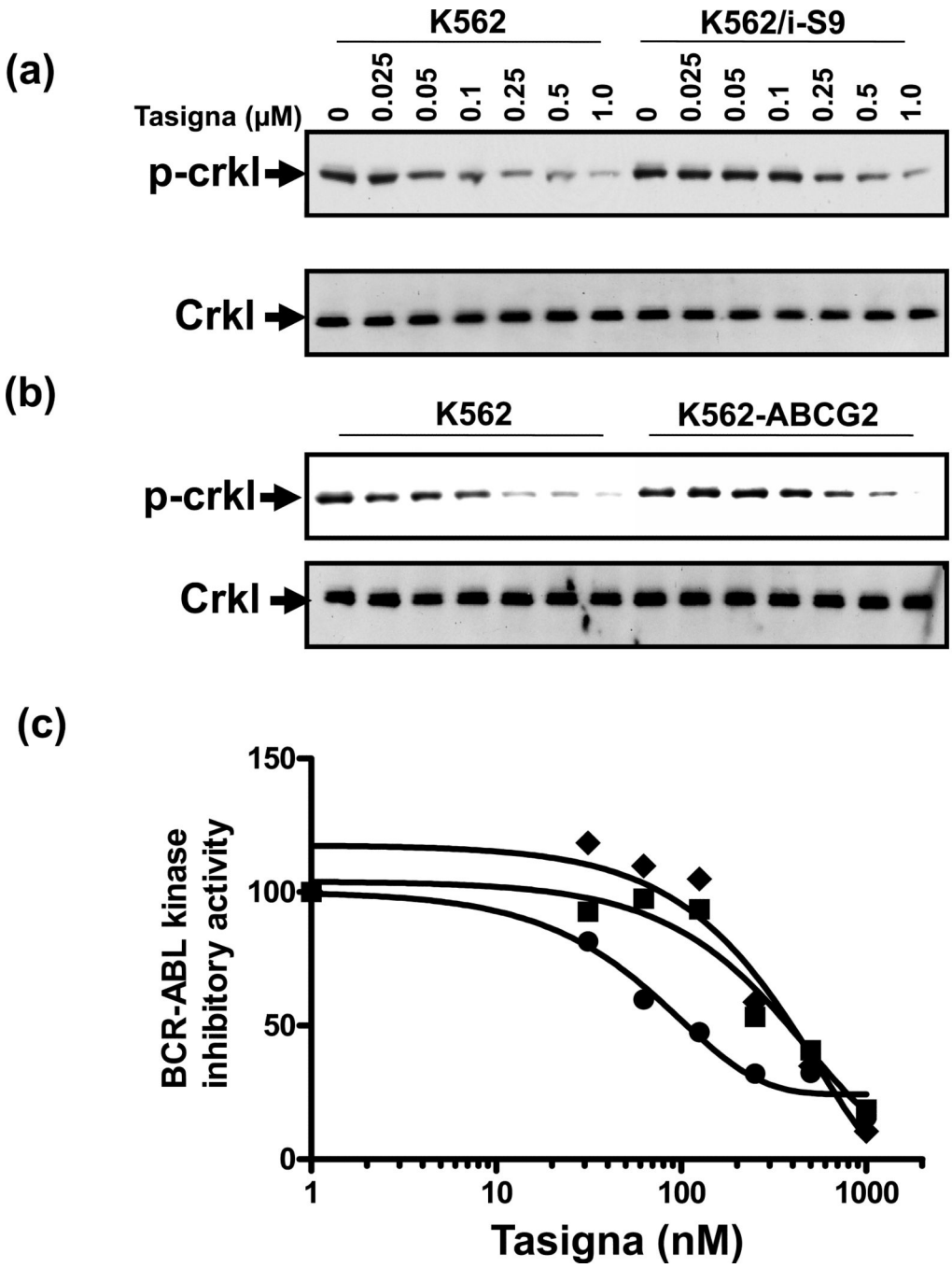

Figure 2. Effect of Tasigna on BCR-ABL kinase activity in Pgp- and ABCG2- expressing K562 cells

K562 (lanes 1-7) in all panels, K562/i-S9 (lanes 8-14 upper panels in a) and K562-ABCG2 (lanes 8-14 upper panel in b), were incubated in the absence (lane 1, 8) or presence of indicated concentrations of Tasigna for 4 h at 37°C. The BCR-ABL kinase activity was measured by monitoring the phosphorylation of P-Crkl (upper panels in a and b) and total Crkl levels (lower panels in a and b) in cell lysates from these cells as described in the Experimental section. Shown here is a representative Western blot detecting P-Crkl and total Crkl levels from a representative experiment. Similar results were obtained in two additional experiments. (c) The P-Crkl level (measurement of BCR-ABL kinase activity) (from

Western blot, Y-axis) in control K562 (●) and K562/i-S9 (■) (Pgp-expressing) or K562-ABCG2 (◆) was quantified by using the ImageQuaNT TL software and plotted as a concentration of Tasigna (X-axis).

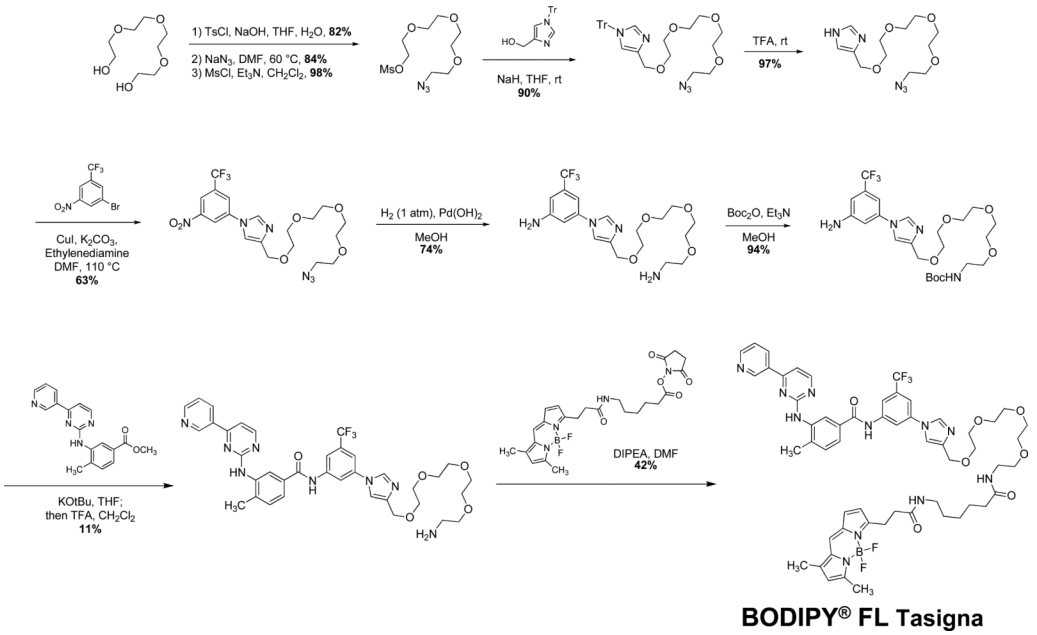

Figure 3. Scheme for synthesis of BODIPY® FL Tasigna

Detailed characterization of intermediates and purity of final product is described in the supplementary data section.

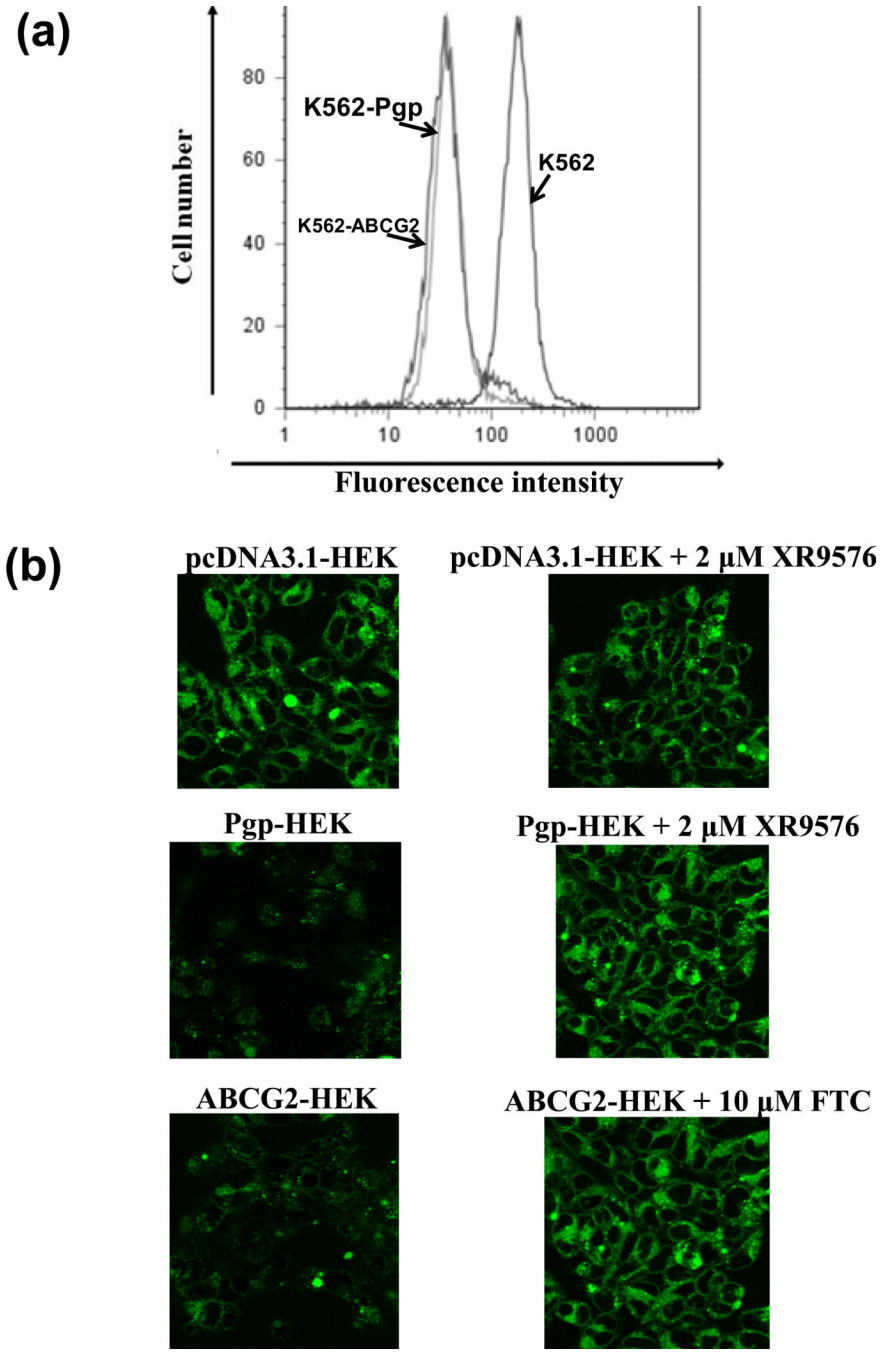

Figure 4. BODIPY® FL Tasigna is transported by both Pgp and ABCG2. (a) BODIPY® FL Tasigna is effluxed by Pgp-expressing K562 cells

K562, K562/i-S9 (Pgp-expressing) or K562-ABCG2 (ABCG2-expressing) cells were incubated with 0.5 μM of BODIPY® FL Tasigna for 45 min at 37°C in the dark, as indicated. The cells were then washed and analyzed by flow cytometer as described in the Experimental section. Similar results were obtained in three additional experiments. (b) Detection of cellular accumulation of BODIPY®-FL Tasigna by confocal microscopy: pcDNA3.1-HEK, Pgp-HEK and ABCG2-HEK cells were incubated with 0.5 μM BODIPY® FL Tasigna in absence (left panels) or presence (right panels) of 2 μM Pgp inhibitor XR9576 or 10 μM ABCG2 inhibitor FTC at 37°C for 45 min. The cells were washed twice with cold

PBS and the images were acquired as described in the Experimental section. Shown here are representative images from one experiment. Similar results were obtained in three additional experiments.

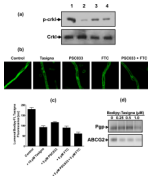

Figure 5. BODIPY® FL Tasigna inhibits BCR-ABL kinase activity

(a, b) K562 cells were incubated in the absence (lane 1) or presence of 1 μM Tasigna (lane 2), 10 μM (lane 3) and 20 μM (lane 4) BODIPY® FL Tasigna for 4 h at 37°C. The BCR-ABL kinase activity was measured by monitoring the phosphorylation of P-Crkl (upper panel) and total Crkl (lower panel) in cell lysates from these cells as described in the Experimental section. BODIPY® FL Tasigna is effluxed by blood-brain barrier capillaries: (b, c) Rat brain capillaries were incubated for 1 h at room temperature in the presence or absence of indicated inhibitors with 2 μM BODIPY® FL Tasigna. Confocal images of 10 capillaries were acquired by confocal microscopy using a 40X oil immersion objective as described in the Experimental section. The images were analyzed by measuring lumenal fluorescence intensity of BODIPY® FL Tasigna (arbitrary units, Y-axis) and plotted as a function of different inhibitors (X-axis). Each data point represents the BODIPY® FL Tasigna fluorescence mean value from 10 capillaries (pooled capillary tissue from 10 rats of a single preparation); variability is given by SEM bars. Units are arbitrary fluorescence units (scale 0-200). (d) BODIPY® FL Tasigna interacts at the substrate-binding pocket of Pgp and ABCG2. Crude membranes (500 μg/ml) from Hi-five Pgp- and ABCG2- expressing cells were incubated with indicated concentrations of BODIPY® FL Tasigna (0-1 μM) for 5 min at 21-23°C in 50 mM Tris-HCl, pH 7.5. 3-6 nM [^{125}I]-IAAP (2200 Ci/mmole) was added and incubated for an additional 5 min under subdued light. The samples were processed as described in the legend to Figure 1c.

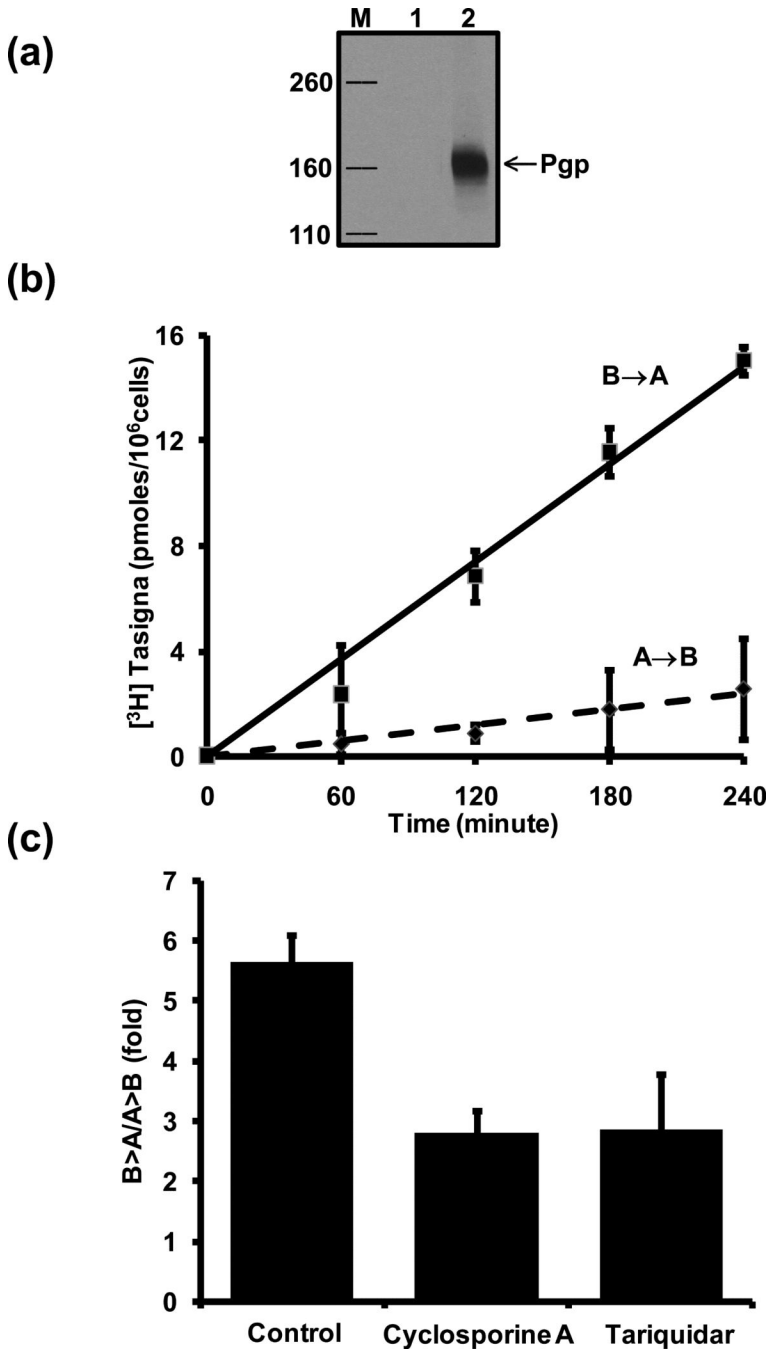

Figure 6. Transepithelial transport of [^{3}H]-Tasigna across monolayers formed by LLC-PK1 cells expressing human Pgp

(a) Expression of human Pgp in LLC-PK1 cells. Total cell lysates from LLC-PK1 (lane1) and LLC-PK1-MDR1 (lane 2) cells were separated by SDS-PAGE. Pgp level was detected with the anti-Pgp (C219) antibody as described in the Experimental Section. Lane M, MW markers (Kda). (b) Efflux of [^{3}H]-Tasigna by Pgp as a function of time. [^{3}H]-Tasigna (64 nM) was added to either the apical or basolateral side of the monolayer. An aliquot (50 μl) of the media was removed from the opposite side of the cell monolayer at indicated time points and processed as described in the Experimental section. The squares show the basolateral-to-apical (B→A) transport, the diamonds show the apical-to-basolateral transport

(A→B). (c) Effect of Pgp-specific inhibitors on transepithelial transport of [^{3}H]-Tasigna. LLC-PK1-Pgp Cell monolayers were incubated with [^{3}H]-Tasigna (64 nM; 1 μCi/ml) in the presence or absence of cyclosporine A (10 μM) and tariquidar (1 μM) for 180 minutes. Directional drug transport ratios across cell monolayers were measured. Each point shows the mean ± SE from at least three independent experiments.

Table 1

Tasigna sensitizes P-glycoprotein-expressing cells to doxorubicin

		IC_{50} [nM][a]		
	Conc. [μM]	**pcDNA-HEK293**	**Pgp-HEK293 (Pgp)**	**RR[b]**
Doxorubicin alone	**-**	11.45 ± 1.60	201.84 ± 45.80	18
+ Tasigna	**1**	12.55 ± 1.66	28.66 ± 6.74	2
+ XR 9576	**1**	11.33 ± 1.29	10.18 ± 1.90	1

[a] IC_{50} values are mean ± SD in the presence and absence of Tasigna or XR9576. The IC_{50} values were calculated from dose-response curves obtained from three independent experiments.

[b] RR (Relative resistance) values were obtained by dividing the IC_{50} values of drug for Pgp-expressing Pgp-HEK293 cells by the IC_{50} values of the parental pcDNA3.1-HEK293 cells in the absence of test drug.